

Probabilistic pairwise sequence alignment

Lawren Smithline

October 29, 2018

Abstract

We describe a new algorithm for visualizing an alignment of biological sequences according to a probabilistic model of evolution. The resulting data array is readily interpreted by the human eye and amenable to digital image techniques.

We present examples using mRNA sequences from mouse and rat: three cytochromes and two zinc finger proteins. The underlying evolutionary model is derived from one proposed by Thorne, Kishino, and Felsenstein and improved by Hein and others. The demonstration implementation aligns two sequences using time and memory quadratic in the mean sequence length.

The algorithm is extensible, after Lunter, Miklós, Song and Hein to multiple sequences. We mention a basic method to reduce time and memory demands.

1 Introduction

The problems of inferring common ancestors and determining the evolution of observed biological sequences have received much attention. The challenge becomes greater with the interest in mining genome scale sequences for meaning. The most popular tools produce mountains of data which are hard to assimilate.

Current solution strategies for sequence alignment begin by postulating some model of evolution in order to score proposed alignments. This transforms the task into development of good score functions and the search for alignments with high score.

The BLAST family of tools uses a hash-and-extend method to find regions of the test sequences which have high similarity, measured by its score model. A hash-and-extend method searches for identical short subsequences by a very fast hash table search and extends these short exact matches to longer not quite exact matches.

Dynamic programming tools, including CLUSTAL, use a score array to find the best scoring global alignment. Needleman-Wunsh and Smith-Waterman are classic algorithms for the two sequence global alignment problem.

Both of these approaches are useful for aligning sequences when the true picture is a one-to-one correspondence, possibly with simple deletions or insertions.

BLAST picks out one-to-many similarities. CLUSTAL finds a one-to-one alignment of whole sequences or alignment profiles. Neither is optimal for the other task.

Both approaches are fooled by sequences which have internal near repeats. This can happen when there are duplications from part of an ancestor sequence in each of its descendants, When the duplications are not identical for each descendant or duplications have independently mutated, there are many regions in one sequence similar to many regions in another. CLUSTAL chooses one path, which maximizes global score, but may have a nonsense agglomeration of gaps. BLAST typically reports every pair of similar subsequences. It is an easy *in silico* demonstration that BLAST can miss similarities entirely if mutations are peppered just frequently enough.

Our goal is to develop an alignment method which finds good global alignments and does not cut out those alignments which score well but not highest.

Merits of our score function are: it is meaningful as a probability; it describes locally the value of an alignment at a point; and it is comparable within an alignment and across alignments. These features permit detection of repeats and duplications.

We concentrate on developing technique for pairwise alignment in a way which is extensible to small numbers of sequences. A larger goal, not yet realized, is multiple genomic alignments. Toward this end, we suggest a conceptually easy way to avoid computing on regions which score so poorly, that they are unlikely to contribute to any of the good alignments. It is mentioned after the algorithm description for clarity of the exposition.

Here is the structure of the paper. Section 2 is a technical summary of the algorithm. Section 3 is the detailed construction. Section 4 presents example applications.

2 Algorithm Summary

We compare two sequences \mathbf{A}, \mathbf{B} , of lengths $l_{\mathbf{A}}$ and $l_{\mathbf{B}}$ using a two dimensional array W . The indices of W range from zero to the length of each sequence.

Denote by $\mathbf{A}[i]$ the letter in position i of sequence \mathbf{A} , and by $\mathbf{A}[i_1, i_2]$ the subsequence of \mathbf{A} from positions i_1 to i_2 .

Our metaphor for comparing \mathbf{A} and \mathbf{B} is writing them on a long paper tape, like CLUSTAL output without line breaks. Number the columns from zero, with the zeroeth position in each row containing a special start symbol, \mathcal{S} . The last column on the tape is filled with a special end symbol, \mathcal{E} . Otherwise, each position may be a letter, A, C, G, T for nucleotide sequences, or a blank, and no column is entirely blank. We model the machine which writes the tape column by column as a Markov process.

A list of transitions for the machine is an evolutionary history and has a probability which is the product of the probability of each transition.

We define the arrays $P(i, j)$, $P^\vee(i, j)$, and $V(i, j)$, with the same indices as W . Let $P(i, j)$ be the probability that the machine writes a tape which can be cut off at some column so that the first row contains \mathcal{S} and $\mathbf{A}[1, i]$ and the second row contains \mathcal{S} and $B[1, j]$, interspersed with any combination of blanks.

This P array produces the [TKF] sum approach when applied with their family of Markov models. Their model gives a sensible way to think of Needleman-Wunsch

dynamic programming summed over all paths, rather than the classic Viterbi trace-back path.

Let $P^\vee(i, j)$ be the probability that the machine writes a tape which can be cut off at some column so that the first row contains $\mathbf{A}[i + 1, l_{\mathbf{A}}]$ followed by \mathcal{E} , and the second row contains $\mathbf{B}[j + 1, l_{\mathbf{B}}]$ followed by \mathcal{E} , with any combination of blanks. We call P^\vee a back fill array and P a front fill array.

Let $\Pi_{\mathbf{A}}$ be the probability for the machine to write a tape with \mathcal{S} followed by \mathbf{A} followed by \mathcal{E} interspersed with blanks in the first row, and $\Pi_{\mathbf{B}}$ be the analog for \mathbf{B} in the second row.

Let

$$V(i, j) = \log \Pi_{\mathbf{A}} + \log \Pi_{\mathbf{B}} - \log P(i, j) - \log P^\vee(i, j).$$

The combination of front fill and back fill makes the values in array V comparable with each other as log likelihoods for the evolutionary process to pass through intermediate points given by coordinates (i, j) . The normalization by $\Pi_{\mathbf{A}}$ and $\Pi_{\mathbf{B}}$ makes V arrays for different sequences comparable. That is, we can answer whether it is more likely \mathbf{A}_1 and \mathbf{B}_1 are related than \mathbf{A}_2 and \mathbf{B}_2 are related.

In the detailed algorithm construction, we modify the TKF process to produce an array W . The concept for the algorithm is the same, but the array $W(i, j)$ weights likelihoods for alignments near position i in \mathbf{A} and j in \mathbf{B} more heavily than positions far away.

3 Algorithm construction

We describe the adaptation of the family of TKF processes to our framework. We refer to the underlying Markov process of [TKF] and [LMSH] as the *ground process*.

3.1 The one state ground process

The ground process is a simple model of evolution. It has predictive strength and permits a clean description of the new algorithm. The ground process is really a complex parameter and a different process may be substituted without essential changes to our algorithm. For example, we could use the process of [TKF2], which allows different substitution models for transitions and transversions.

The ground process evolution model is that beginning with an ancestor sequence \mathbf{C} , the sequence of each generation is mostly copied faithfully to the next generation, and occasionally letters are substituted, deleted, or inserted. The frequency of these events is expressed per letter, per evolutionary distance, i.e. time.

The ground process is reversible. The probability for a particular letter at a certain point to be deleted is the same as the probability to insert that particular letter at a that point. Substitution of letter X for letter Y has the same probability as the reverse substitution.

For sequences \mathbf{A} and \mathbf{B} , let

$$Pr_t(\mathbf{A}, \mathbf{B})$$

be the probability that \mathbf{A} and \mathbf{B} are separated by evolutionary distance t , and so diverged $t/2$ ago. Let

$$Pr_t(\mathbf{B}|\mathbf{A})$$

be the probability that \mathbf{A} evolves to \mathbf{B} over evolutionary distance t . In this view, $\Pi_{\mathbf{A}}$ is the equilibrium probability to observe \mathbf{A} after a long time and $\Pi_{\mathbf{B}}$ the equilibrium probability to observe \mathbf{B} .

A consequence of reversibility is

$$Pr_t(\mathbf{A}, \mathbf{B}) = \Pi_{\mathbf{A}} Pr_t(\mathbf{B}|\mathbf{A}) = \Pi_{\mathbf{B}} Pr_t(\mathbf{A}|\mathbf{B}).$$

Thus, it is unnecessary to find the hidden ancestor of \mathbf{A} and \mathbf{B} in order to evaluate their similarity.

We describe the ground process in two parts: the development of an evolutionary history, and the specification of the letters which fill that history.

The start state of the machine writes column zero $\begin{smallmatrix} \mathcal{S} \\ \mathcal{S} \end{smallmatrix}$, on the paper tape, expressed as the ordered pair $(\mathcal{S}, \mathcal{S})$. The transition to each state writes a column on the paper tape, using \mathcal{N} to stand in for a nucleotide to be selected in the next phase. The available states and their transition outputs are: homology, $(\mathcal{N}, \mathcal{N})$; deletion, $(\mathcal{N}, -)$; insertion, $(-, \mathcal{N})$; and termination, $(\mathcal{E}, \mathcal{E})$. A nonhomology event, including mismatch, is deletion followed by insertion.

An evolutionary history is a sequence of transitions beginning at start and ending at termination. Define the *fate* of a nonblank symbol in the \mathbf{A} sequence (top or first member of pair) as the sequence of columns beginning with that symbol and ending just before the column with the next nonblank symbol in the \mathbf{A} sequence. The fate of \mathcal{S} is start followed by some number of insertions. The fate of \mathcal{N} is either homology or deletion followed by some number of insertions. The fate of \mathcal{E} is termination.

The parameters for determining the probability of an evolutionary history according to a ground process are the insertion rate λ expressed per base per time, the deletion rate μ , and the evolutionary distance t . We compute the probabilities using the limit for large K of a discrete process with insertion rate $\lambda t/K$ per base, deletion rate $\mu t/K$ per base. The resulting probabilities are expressions in $l = \lambda t$ and $m = \mu t$.

Let

$$B = \frac{l - le^{l-m}}{m - le^{l-m}}.$$

Let

$$\alpha = l/m.$$

(This B is $\lambda\beta(t)$ in [TKF], and α is $\lambda\beta(\infty)$.)

The probability for \mathcal{S} to be part of an evolutionary history with k insertions is

$$(1 - B)B^k.$$

The probability to extend \mathbf{A} by another letter is α . The probability to transition to end is $1 - \alpha$.

Given that \mathbf{A} is extended by another letter, we have the following probabilities. The probability for homology followed by zero insertions is

$$H = e^{-m}(1 - B).$$

The probability for homology followed by k insertions is

$$HB^k.$$

The probability for deletion followed by zero insertions is

$$E = B/\alpha.$$

The probability for deletion followed by exactly one insertion is

$$N = (1 - e^{-m} - E)(1 - B).$$

The probability for deletion followed by $k > 1$ insertions is NB^{k-1} .

For the start and homology events, every successive insertion is with probability B , but for a deletion event, the probability of the first insertion is different. The ground process in [TKF] is presented as a machine with a deletion state that has different transition probabilities from the other states for this possible first insertion.

The insight of [HWKMW], extended in [LMSH], is the description of the ground process using one main state and multiple transitions, including a “forbidden transition” with negative transition factor to accomplish the same result. The forbidden transition is from a deletion event with zero insertions to an insertion event.

The evolutionary history is completed to a sequence alignment by writing a letter from the alphabet A, C, G, T in place of each \mathcal{N} .

The ground process has parameters $\pi_A, \pi_C, \pi_G, \pi_T$ which define a distribution of letters. The parameter σ determines the substitution rate per base per time. As above, the equations can be expressed in terms of $s = \sigma t$.

The probability for an insertion or deletion process to produce a letter X is π_X . For a homology event, the probability for the ground process to produce the pair (X, Y) is $\pi_X f(X, Y)$, where

$$f(X, Y) = (1 - e^s)\pi_Y + \delta_{X,Y}e^s,$$

and $\delta_{X,Y}$ is one or zero depending on whether X and Y are the same.

The computation of the array $P(i, j)$ for sequences \mathbf{A} and \mathbf{B} is recursive. The base cases are P with either index negative is zero and

$$P(0, 0) = 1 - B.$$

Thereafter,

$$\begin{aligned} P(i, j) = & P(i-1, j) \cdot B\pi_{\mathbf{A}[i]} + P(i, j-1) \cdot B\pi_{\mathbf{B}[j]} + \\ & P(i-1, j-1) \cdot \alpha\pi_{\mathbf{A}[i]}(N\pi_{\mathbf{B}[j]} + Hf(\mathbf{A}[i], \mathbf{B}[j])) - \\ & P(i-1, j-1) \cdot B^2\pi_{\mathbf{A}[i]}\pi_{\mathbf{B}[j]}. \end{aligned}$$

The probability to observe \mathbf{A} and \mathbf{B} related by some evolutionary history is $(1 - \alpha)P(l_{\mathbf{A}}, l_{\mathbf{B}})$.

3.2 Modifying the one state ground process

We modify the computation of the array P to compute a related array Q .

We consider further implications of the reversibility of the ground process. The parameters l and m are *a priori* two degrees of freedom in the ground process. If the lengths of \mathbf{A} and \mathbf{B} are informative, setting l and m to maximize the probability to observe sequences of the given lengths gives a relationship between l and m . We choose m and derive l .

If the sequences \mathbf{A} and \mathbf{B} are subsequences of very very long genomes, the lengths of \mathbf{A} and \mathbf{B} may be artifacts of truncation. We express this in the ground process by $l = m$, making insertions and deletions equally likely. In this case, extension of \mathbf{A} is a zero information event, expressed by $\alpha = 1$. Other transition probabilities are computed in terms of

$$B = l/(1 + l).$$

Gaps at the ends of alignments could be artifacts of truncation. We model this by replacing B by α at the edges of the P array. This models extending the sequences in each direction infinitely with bases selected from distribution π .

We normalize by dividing by the probability to observe sequences \mathbf{A} and \mathbf{B} separately given l , m , and π and omitting the factor for the initial state $1 - B$. We report separately the log likelihood to observe the given sequences,

$$\log \Pi_{\mathbf{A}} + \log \Pi_{\mathbf{B}}.$$

Assembling the above insights, we compute

$$\begin{aligned} Q(0,0) &= 1, \\ Q(i,0) &= Q(i-1,0), \\ Q(i,j) &= Q(i-1,j) \cdot E + Q(i,j-1) \cdot E + \\ &\quad Q(i-1,j-1)(N + Hf(\mathbf{A}[i], \mathbf{B}[j])/\pi_{B[j]}) - \\ &\quad Q(i-1,j-1) \cdot E^2, \\ Q(i, l_{\mathbf{B}}) &= Q(i-1, l_{\mathbf{B}}) + Q(i, l_{\mathbf{B}}-1) \cdot E + \\ &\quad Q(i-1, l_{\mathbf{B}}-1)(N + Hf(\mathbf{A}[i], \mathbf{B}[l_{\mathbf{B}}])/\pi_{B[l_{\mathbf{B}}]}) - \\ &\quad Q(i-1, l_{\mathbf{B}}-1) \cdot E^2. \end{aligned}$$

We do not multiply the final entry by $1 - \alpha$, because we are not asserting the sequences end.

The Q array provides the same kind of information as the P . The essential difference is that the gap cost for leading and trailing gaps is canceled. It is possible to treat gaps differently along each edge of the array.

3.3 New constructions for visualization

Computing evolutionary history using the sequences \mathbf{A} reversed and \mathbf{B} reversed is computationally the same problem as for \mathbf{A} and \mathbf{B} as given.

Let $P^\vee(i, j)$ be the probability for the sequences $\mathbf{A}[i+1..l_{\mathbf{A}}]$ and $\mathbf{B}[j+1, l_{\mathbf{B}}]$ to align by some evolutionary history. Let $Q^\vee(i, j)$ be $P^\vee(i, j)$ normalized by the probability to observe the given sequences.

The base cases are

$$\begin{aligned} P^\vee(l_{\mathbf{A}}, l_{\mathbf{B}}) &= 1, \\ Q^\vee(l_{\mathbf{A}}, l_{\mathbf{B}}) &= 1. \end{aligned}$$

The equations for $P^\vee(i, j)$ and $Q^\vee(i, j)$ are the same as those for P and Q , except progress is towards $i = 0, j = 0$ rather than away.

The product $P(i, j)P^\vee(i, j)$ is the probability \mathbf{A} and \mathbf{B} arose from some evolutionary history which restricts to an evolutionary history for $\mathbf{A}[1, i]$ and $\mathbf{B}[1, j]$, and for $\mathbf{A}[i+1, l_{\mathbf{A}}]$ and $\mathbf{B}[j+1, l_{\mathbf{B}}]$

Let

$$R(i, j) = Q(i, j)Q^\vee(i, j).$$

The entry $R(i, j)$ is the probability for an evolutionary history as for $P(i, j)P^\vee(i, j)$, providing for the artifactual truncation of sequence, divided by the probability that the sequences \mathbf{A} and \mathbf{B} were observed and the evolutionary history is start, $l_{\mathbf{A}}$ deletions followed by $l_{\mathbf{B}}$ insertions, end.

Every entry in $R(i, j)$ is comparable to every other entry. The contours near the maximum value of $R(i, j)$ bound the region containing the paths of the most likely alignments.

We propose another pair of arrays $S(i, j)$ and $S^\vee(i, j)$ which weight recent history more than distant history. We adapt the standard technique of approximating a sliding window by multiplying an accumulator by a factor between zero and one, and adding the new data value. An alternative interpretation is that we view the developing evolutionary history through a fog which makes distant states uncertain. The thickness of the historical fog is a parameter ρ . The generic computation for S is

$$\begin{aligned} S(i, j) &= \rho + (1 - \rho)S(i - 1, j) \cdot E + \\ &\quad (1 - \rho)S(i, j - 1) \cdot E + \\ &\quad (1 - \rho)S(i - 1, j - 1)(N + Hf(\mathbf{A}[i], \mathbf{B}[j])/\pi_{B[j]}) - \\ &\quad (1 - \rho)^2 S(i - 1, j - 1) \cdot E^2, \end{aligned}$$

with suitable modifications at the boundaries.

Another model with the same mathematical description is that with probability $\rho \Pi_{\mathbf{A}[1, i]} \Pi_{\mathbf{B}[1, j]}$ the subsequences $\mathbf{A}[1, i]$ and $\mathbf{B}[1, j]$ are observed and discarded from consideration in the evolutionary history. The Smith-Waterman algorithm is a Viterbi path application of the similar idea that the alignment process might have optimal score applied to subsequences of \mathbf{A} and \mathbf{B} .

We use the parameter

$$r = \rho^{-1} - 1.$$

From the view of ρ as the probability of a jump event, we call r the odds against a jump event.

When $r = \infty$, and the other parameters are equal,

$$Q(i, j) = S(i, j).$$

We implement the computations

$$\begin{aligned} J(i, j) &= -\log S(i, j), \\ J^\vee(i, j) &= -\log S^\vee(i, j), \\ W(i, j) &= J(i, j) + J^\vee(i, j). \end{aligned}$$

We also compute the equilibrium value ν for noise given parameters l, m, r, s and distribution π . This is the limit for large i, j of $J(i, j)$ for long random sequences constructed from distribution π .

Using ν , we can approximate $W(i, j)$ in any shape region by clamping the boundary values of $J(i, j)$ and $J^\vee(i, j)$ equal to ν when they are not otherwise actually calculated. This makes sense, for example, when we want to avoid computing on an area where we believe there is no alignment and want results for an adjacent area. We can also mask out a high scoring evolutionary history by forcing $J(i, j) = \nu$ on its path. This allows a second place ridge to be seen as maximum.

4 Application of the W array

Computing W requires the sequences \mathbf{A} and \mathbf{B} , the parameters insertion rate l , deletion rate m , substitution rate s and jump odds r , and the distribution π .

In the examples below, we fix $l = m$, and take π to be the distribution observed in the sequences \mathbf{A} and \mathbf{B} . We handle the nucleotide symbol N as a match for each nucleotide A, C, G, T with distribution π .

In principle, these parameters can be dynamically reestimated for different points in the array. Also, a global maximum likelihood reestimation can be done in the manner of the [TKF] sum approach.

We compute, but do not apply, the noise value ν .

We apply a simple digital image technique to find the local extreme contours. We compute $W(i, j)$ and plot, on a grayscale, the difference

$$\Delta W(i, j) = W(i + 1, j) - W(i, j + 1).$$

In Section 4.1, we show an example of finding evolutionary distance by using $r = \infty$ and simple reestimation of s . We show an example of curating sequences with repeats and duplications.

Note in the following examples the black and white diamonds in the plots of ΔW . These occur at places where segments of the two sequences, represented on the horizontal and vertical axes, align with high identity. The sharp contrast along the diagonal of the diamond indicates a local extreme contour in the W array. The intensity of

a sequence identity feature in the W array is proportional to its length. The longest identity feature has maximum intensity and depresses the intensity of other identity features. In the ΔW array, the width of an identity feature is proportional to its length, and its intensity is not affected by its length. Thus, ΔW shows different length identity features simultaneously.

4.1 Comparison of three rodent cytochromes

We compare the mRNA sequences for proteins *Rattus norvegicus* cytochrome P450 IIA1 and IIA2, (Cyp2a1 and Cyp2a2), from [MNKG], and *Mus musculus* cytochrome P450, IIA12 (Cyp2a12), from [ILJN].

Figure 1 shows a grayscale plot $\Delta W(i, j)$ for sequences Rn-Cyp2a1 and Mm-Cyp2a12 using the parameters $m = s = 0.1$ and $r = 4$. From this picture, we can infer that the evolutionary history between these sequences contains no jump events. Thus, we set $r = \infty$ for further iterations. We also see no deletion events, so we decrease m .

Figure 2 shows a grayscale plot of $\Delta W(i, j)$ with parameters $m = s = 0.03$, $r = \infty$. We perform this computation for all three pairs of sequences. For the following pairs, we calculated the difference between the maximum and minimum of the W array.

Mm-Cyp2a12	Rn-Cyp2a1	2263
Mm-Cyp2a12	Rn-Cyp2a2	2110
Rn-Cyp2a1	Rn-Cyp2a2	2398
Mm-Cyp2a12	Mm-Cyp2a12	2844

We expect two random sequences to be about 27% identical. The value is greater than 25%, because the distribution of nucleotides π is not flat. We know Mm-Cyp2a12 is 100% identical to itself. By dividing 73% into 2844, we find that a difference of 38 units of log-likelihood represents 1% of sequence identity for these sequences and parameters.

We estimate the following sequence divergences:

Mm-Cyp2a12	Rn-Cyp2a1	14.9%
Mm-Cyp2a12	Rn-Cyp2a2	18.8%
Rn-Cyp2a1	Rn-Cyp2a2	11.4%

We compute arrays with new parameters. We maintain $r = \infty$. We set $m = 10^{-6}$. We set s to be the whole number percentages near the values computed above. The plots of ΔW are similar to those for figures 1 and 2. The values of s which produce the maximum log-likelihoods are:

Mm-Cyp2a12	Rn-Cyp2a1	14%
Mm-Cyp2a12	Rn-Cyp2a2	17%
Rn-Cyp2a1	Rn-Cyp2a2	11%

4.2 Comparison of two zinc finger proteins

We compare two zinc finger proteins from *Mus musculus*. We use the mRNA sequences for Zfp111 and Zfp235 [SHGBS]. These two proteins have a similar amino

acid sequences: one KRAB domain, followed by a spacer region, followed by a series of zinc finger domains in tandem. The members of this protein family each have from five to nineteen of the 28 amino acid zinc finger domains. Most of these amino acids are required for zinc binding, and are highly conserved between duplications and between genes. Shannon et al. show statistically that over all nucleotide positions in the zinc finger domains, substitution events tend to be synonymous. They observe a range of selection behaviors at positions believed to be noncritical to the zinc binding function.

Figure 3 shows the W array computed with the Zfp111 and Zfp235 sequences. The W array shows high sequence identity at the beginning of the sequence, followed by a mismatch with a net insertion in the Zfp235 sequence.

Figure 4 shows the ΔW plot for the same sequences and parameters. The ΔW plot provides more detail on the mismatch discovered by the W array plot. We see insertion of the second Zfp235 zinc finger relative to Zfp111 and insertion of either the eighth or ninth Zfp111 zinc finger relative to Zfp235.

Figure 5 shows a detail of the same ΔW array. We can locate a single amino acid deletion in Zfp111 relative to Zfp235.

Zinc fingers 10 through 13 of Zfp235 match zinc fingers 10 through 13 and also zinc fingers 14 through 17 of Zfp111. Figure 6, showing the ΔW array for Zfp111 against itself, provides strong evidence of the internal duplication in Zfp111.

5 Acknowledgment

We thank Rick Durrett for suggesting the examples.

References

- [H] Hein, J., “An algorithm for statistical alignment of sequences related by a binary tree.” *Pac. Symp. Comput.* 2001: 179–190.
- [HWKMW] Hein, J, C. Wiuf, B. Knudsen, M. B. Møller, and G. Wibling, “Statistical alignment: computational properties, homology testing and goodness-of-fit.” *J. Mol. Biol.* 302:265–279 (2000).
- [ILJN] Iwasaki, M., R. L. Lindberg, R. O. Juvonen, and M. Negishi, “Site-directed mutagenesis of mouse steroid 7 alpha-hydroxylase (cytochrome P-450(7) alpha): role of residue-209 in determining steroid-cytochrome P-450 interaction.” *Biochem. J.* 291 (Pt 2): 569–573 (1993).
- [LMSH] Lunter, G. A., I. Miklós, Y. S. Song, and J. Hein, “An efficient algorithm for statistical multiple alignment on arbitrary phylogenetic trees.” Preprint (April 2003).
- [MNKG] Matsunaga, T., M. Nomoto, C. A. Kozak, and F. J. Gonzalez, “Structure and in vitro transcription of the rat CYP2A1 and CYP2A2 genes and regional localization of the CYP2A gene subfamily on mouse chromosome 7.” *Biochemistry* 29 (5):1329-1341 (1990).
- [SHGBS] Shannon, M., T. A. Hamilton, L. Gordon, E. Branscomb, and L. Stubbs, “Differential expansion of zinc-finger transcription factor loci in homologous human and mouse gene clusters.” *Genome Res.* 13 (6A): 1097-1110 (2003).
- [TKF] Thorne, J. L, H. Kishino, and J. Felsenstein, “An evolutionary model for maximum likelihood alignment of DNA sequences.” *J Mol Evol.* 33(2):114–124 (August 1991).
- [TKF2] Thorne, J. L, H. Kishino, and J. Felsenstein, “Inching toward Reality: an improved likelihood model of sequence evolution.” *J Mol Evol.* 34(1):3–16 (January 1992).

Department of Mathematics
Malott Hall
Cornell University
Ithaca, NY 14853
USA

lawren@math.cornell.edu

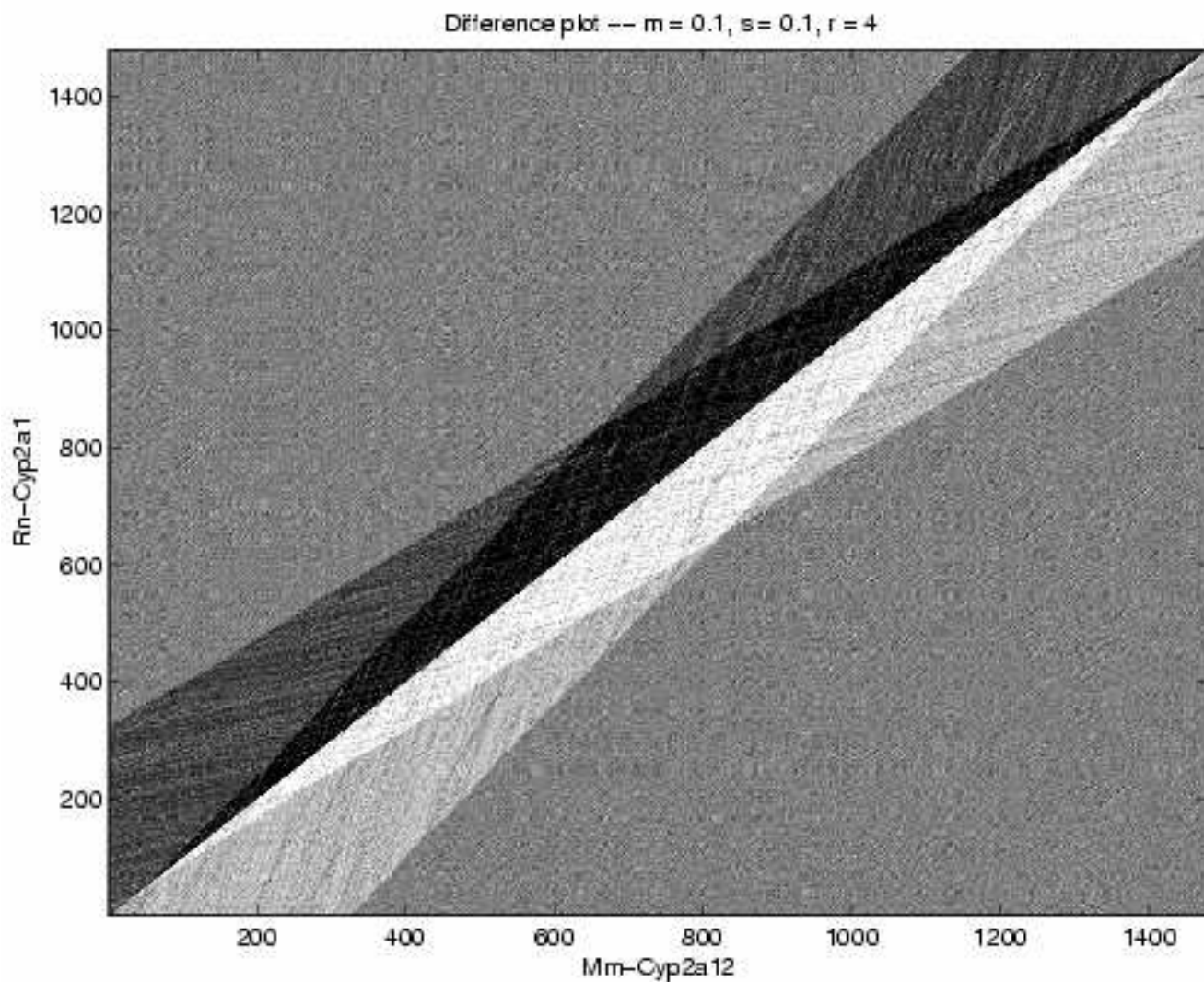


Figure 1: Comparison of cytochromes Rn-Cyp2a1 and Mm-Cyp2a12. We show the log likelihood difference ΔW in grayscale. Qualitatively, the other pairwise comparisons, with Rn-Cyp2a2, look the same. The unique sharp diagonal boundary between black and white triangles shows the best alignment, which far surpasses any alternative model.

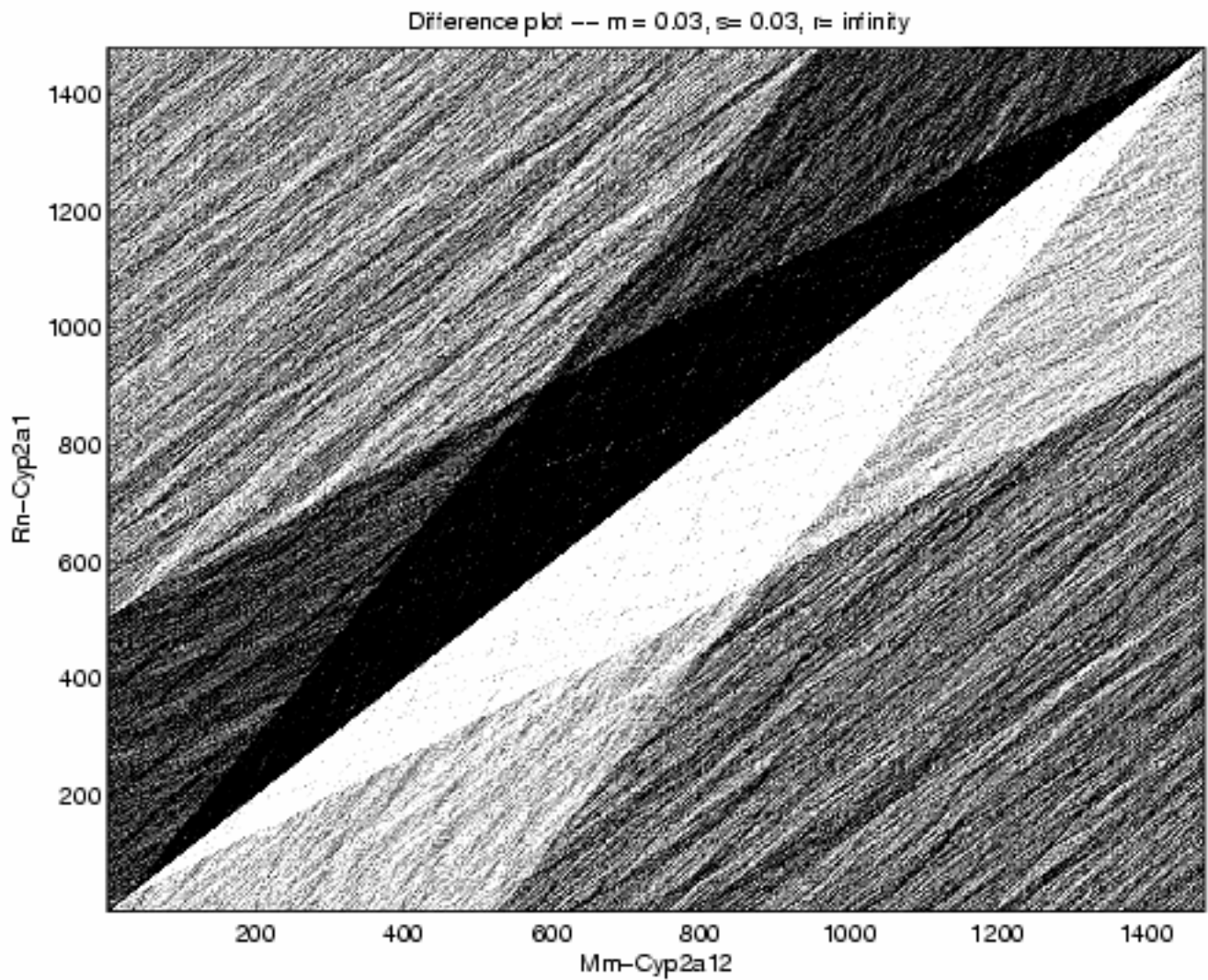


Figure 2: Comparison of cytochromes Rn-Cyp2a1 and Mm-Cyp2a12, with parameters derived from the no jump, no deletion hypothesis, $r = \infty$, decreased m from figure 1. We show the log likelihood difference ΔW in grayscale.

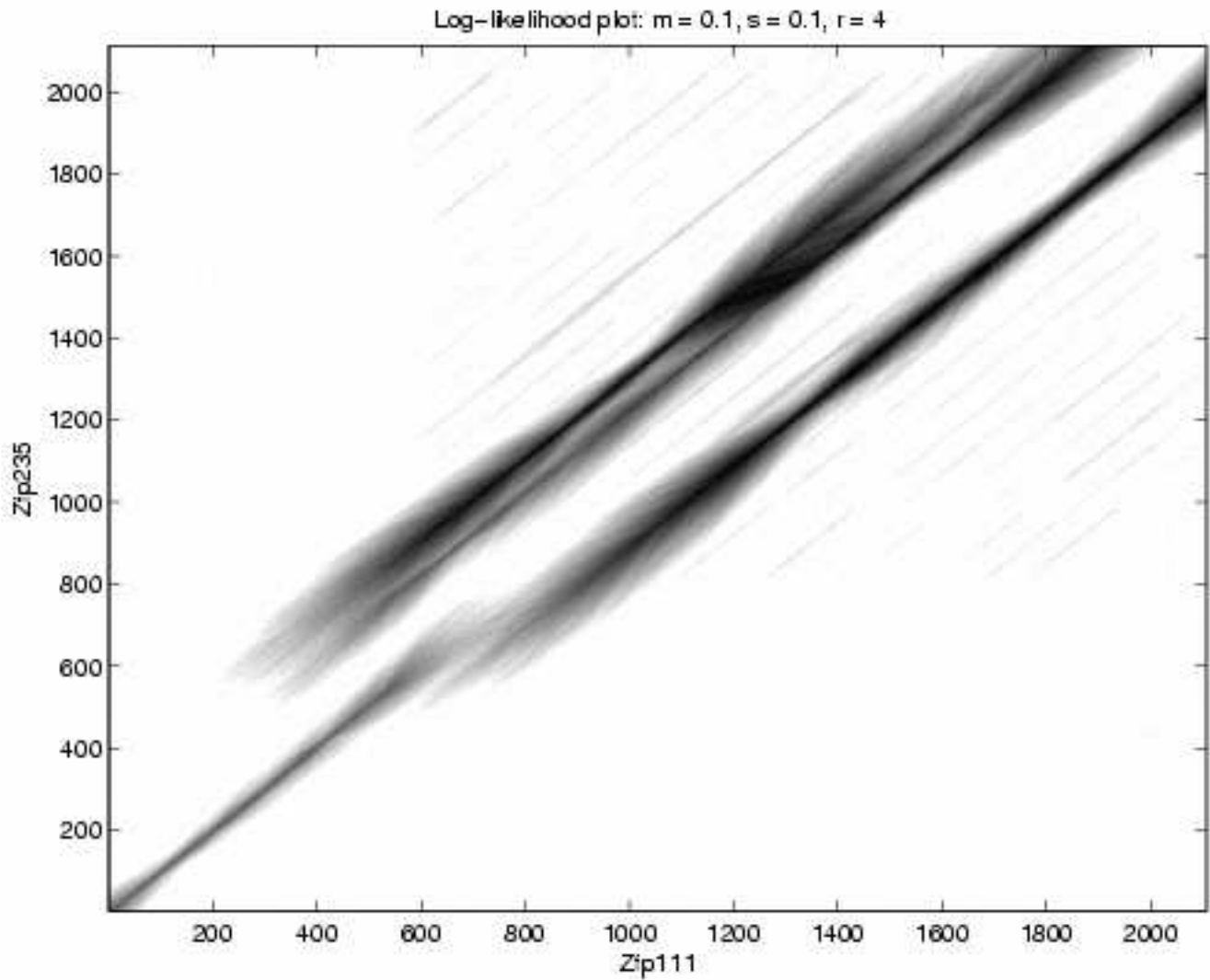


Figure 3: Comparison of zinc finger protein mRNA sequences for *Mus musculus* Zfp111 and Zfp235. The normalized likelihood array W shows: high sequence identity to coordinate (537, 540), then a mismatch with a net insertion of 222 bases in Zfp235. In the rectangle with bottom left corner (622, 844) and top right corner (2106, 2112), there are many parallel tracks, with parts of three more intense than the others.

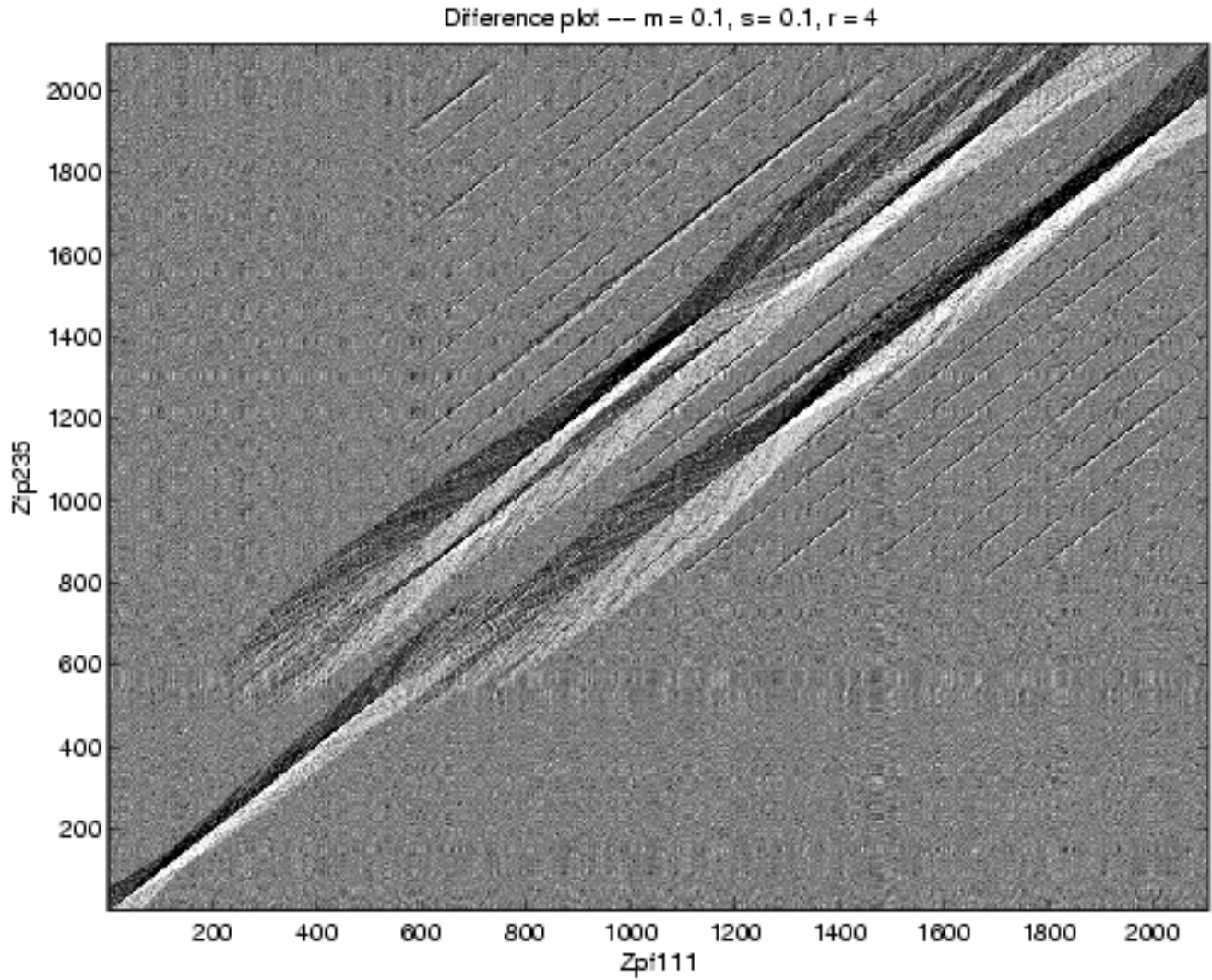


Figure 4: Difference plot ΔW from comparison of Zfp111 and Zfp235. The ΔW array suggests there is high sequence identity between bases 547 through 621 of Zfp111 and 722 through 843 of Zfp235 relative to any potential alignment of these two sequences, by the narrow black and white diamond at these coordinates. Above and to the right of coordinate (622, 844), the parallel tracks suggest near-repeat subsequences and the black and white diamonds indicate the more similar regions. The diamonds which cover the same vertical coordinates, near coordinates 1300 and 1800 of Zfp235, suggest sequence duplication within Zfp111.

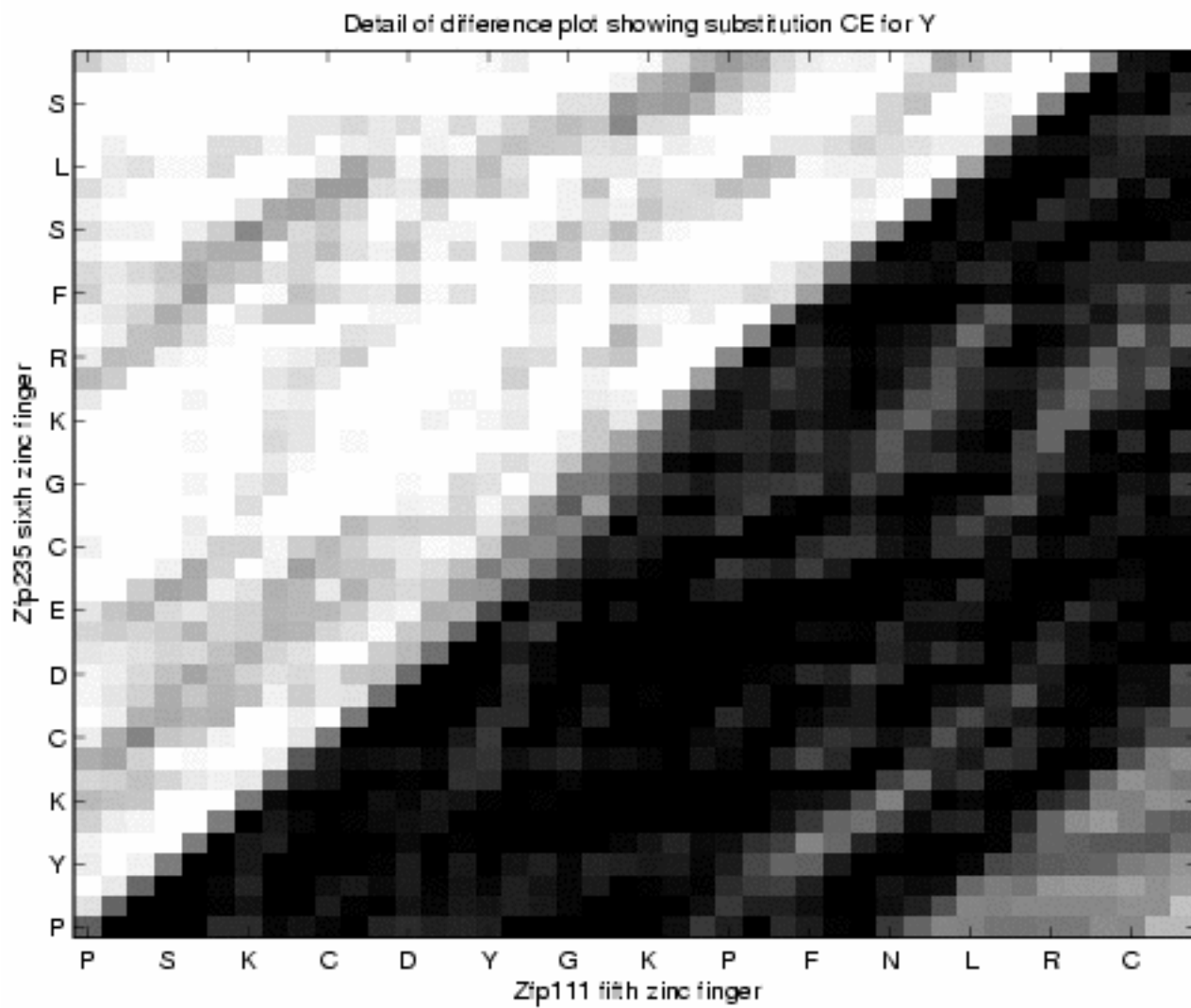


Figure 5: Detail of ΔW showing single amino acid deletion of either the sixth or seventh amino acid of the fifth zinc finger in Zfp111.

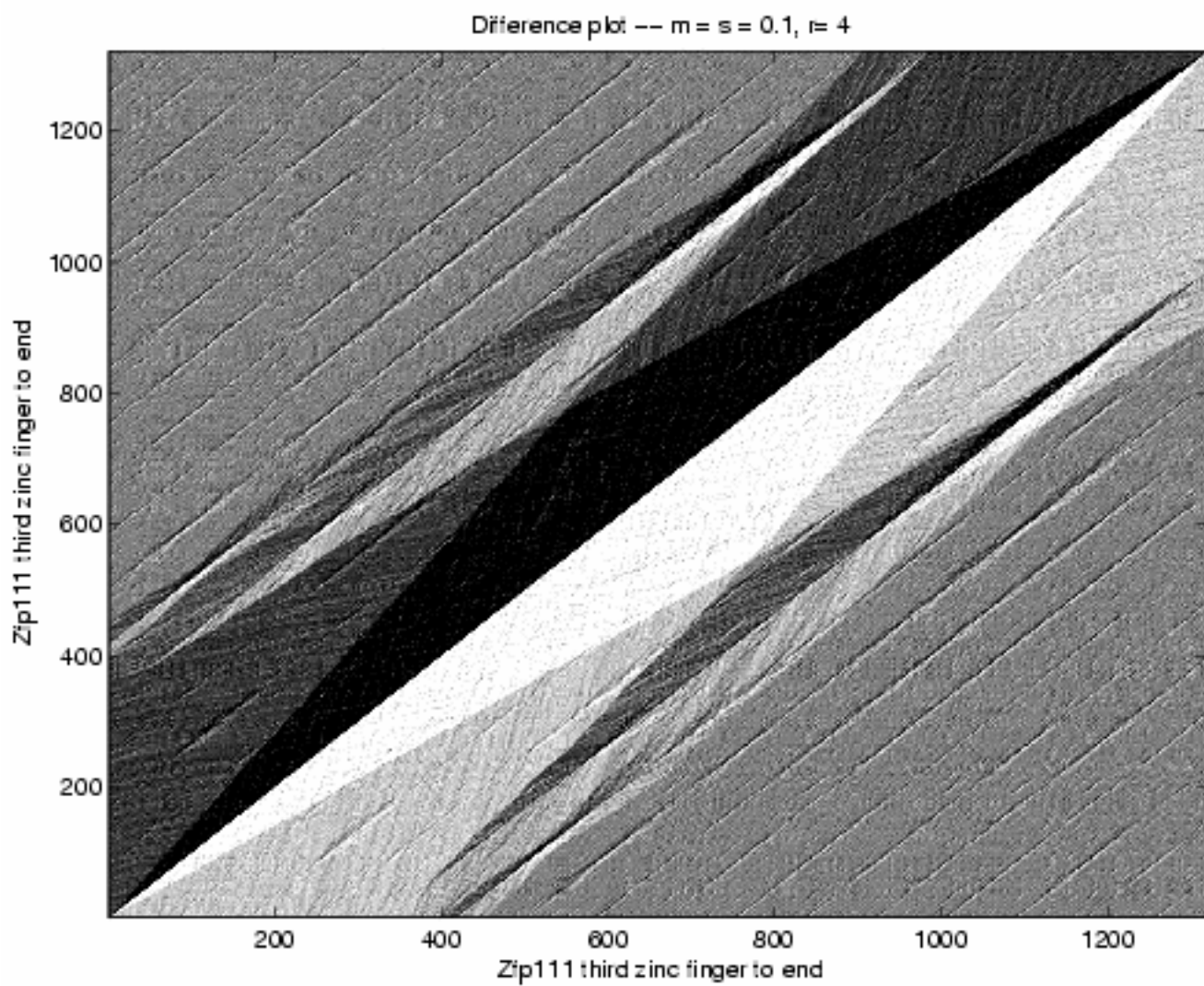


Figure 6: The ΔW array of Zfp111 compared with itself. The black and white diamonds off the large one, centered near coordinates (700, 1100) and (1100, 700) strongly suggest internal duplication.